

# An investigation of the effect of intermediate layer in three-component planar photonic crystal waveguides

HONGJUN SHEN<sup>1, 2\*</sup>, HUIPING TIAN<sup>1</sup>, YUEFENG JI<sup>1</sup>

<sup>1</sup>Key Laboratory of Optical Communication and Lightwave Technologies, Ministry of Education, School of Telecommunication Engineering, Beijing University of Posts and Telecommunications, Beijing 100876, P.R. China

<sup>2</sup>School of Physics and Electrical Information Science of Ningxia University, Yinchuan, 750021, P.R. China

\*Corresponding author: shenhongj2008@hotmail.com

The introduction of a third component into planar photonic crystal waveguides definitely influences the properties of linear defect modes, such as the band diagram, intrinsic loss, group velocity and group velocity dispersion. With the increase of the dielectric constant of the interlayer, the guided modes shift to lower frequencies and the radiative losses decrease in the frequency region of high group velocity of defect mode. The analysis of the sensitivity of a band diagram to the introduction of an interlayer reveals that the wider the planar photonic crystal waveguide and the thicker the slab, the more tolerant the overall structure. When one designs the real planar photonic crystal waveguides, the effect of unintentional intermediate layer on the optical properties of planar photonic crystal waveguides has to be taken into consideration. At the same time, the introduction of an intentional interlayer into macroporous planar photonic crystal waveguides can be utilized to optimize the design.

Keywords: three-component planar photonic crystal waveguide, intermediate layer, group velocity, group velocity dispersion.

## 1. Introduction

As a potential basic building block for integrated optics, planar photonic crystal waveguide (PPCW) is extensively investigated [1–5]. In these systems, there exist two kinds of modes: truly- and quasi-guided eigenmodes. Truly-guided modes lie below the light line and are theoretically lossless, whereas the quasi-guided modes lie above the light line and are subject to intrinsic radiation losses due to out-of-plane diffraction, so the problem of light line restricts the usage of the PPCW. In addition to the problem of light line, a lot of extrinsic factors, such as insufficient etch depth [6], disorder-induced [4, 7, 8], roughness-induced [9], *etc.*, may contribute to radiative losses.

The sensitivity of the PPCW to the fabrication imperfection is a disadvantage in application. Understanding the effects of the imperfection is thus a topic of both fundamental and practical importance and the effects of the imperfection have to be investigated quantitatively.

In this work, a theoretical treatment of the effect of another kind of fabrication imperfection in PPCW is presented. In the fabrication process of macroporous PPCW by the method of electrochemical etching [10], a third medium with dielectric constant  $\varepsilon_i$ , which is different from the bulk ones, is introduced like a ring-shaped intermediate layer around the hole's surface. As a matter of fact, the introduction of the interlayer not only happens in the fabrication process of the PPCW, but also in the practical application it is inevitable. If PPCW does not work in a vacuum, the photonic crystal's "atoms" may slightly change their properties near the interfaces due to some chemical processes (for example oxidization). The inner pore's surface of a macroporous slab structure inevitably contains the interlayer.

The unintentional intermediate layer sensitively affects the properties of PPCW. But up to date, little work has been done about this problem. To our knowledge, only the work of GLUSHKO and KARACHEVTSEVA [10] focuses on the problem in two-dimensional ideal photonic crystals, which are actually unsuitable for practical application. In order to better understand the optical properties of PPCW, it is necessary to investigate the dependence of the properties of PPCW on various structural parameters, which include those of the intermediate layer.

On the other hand, intentional oxidization of the macroporous structure is widely used [11]. For PPCW, the introduction of the extra component enlarges our freedom for fine-tuning of the dispersion properties of PPCW. As a matter of fact, the fabrication of PPCW which allows to tune the photonic band gap edges by an external influence has been one of important directions of investigations [11, 12].

## 2. Theoretical model

For a periodic dielectric constant  $\varepsilon(\mathbf{r})$ , a Bloch state for the magnetic field at the  $n$ -th band and wave vector  $\mathbf{k}$  satisfies the Maxwell equation

$$c^2 \nabla \times \left[ \varepsilon^{-1}(\mathbf{r}) \nabla \times H_{nk}(\mathbf{r}) \right] = \omega_{nk}^2 H_{nk}(\mathbf{r}) \quad (1)$$

$\omega_{nk}$  and  $H_{nk}(\mathbf{r})$  are the eigenfrequencies and eigenvectors, respectively. After insertion of a third component, the new dielectric function, eigenfrequencies and eigenvectors are denoted as  $\tilde{\varepsilon}(\mathbf{r})$ ,  $\tilde{\omega}_{nk}$  and  $\tilde{H}_{nk}(\mathbf{r})$ , respectively. Ignoring the higher order terms, from perturbation theory, it is easy to obtain from Eq. (1) that

$$\begin{aligned} \nabla \times \varepsilon^{-1}(\mathbf{r}) \nabla \times \delta H_{nk} + \nabla \times \left[ \tilde{\varepsilon}^{-1}(\mathbf{r}) - \varepsilon^{-1}(\mathbf{r}) \right] \nabla \times H_{nk}(\mathbf{r}) &\cong \\ \cong \frac{\tilde{\omega}_{nk}^2 - \omega_{nk}^2}{c^2} H_{nk} + \frac{\omega_{nk}^2}{c^2} \delta H_{nk} &\quad (2) \end{aligned}$$

where  $\tilde{H}_{nk} = H_{nk} + \delta H_{nk}$ . By some mathematic strategies [13], we finally obtain

$$\left(\frac{\tilde{\omega}_{nk}}{\omega_{nk}}\right)^2 - 1 \approx \frac{\int [\tilde{\epsilon}^{-1}(\mathbf{r}) - \epsilon^{-1}(\mathbf{r})] |D_{nk}(\mathbf{r})|^2 d\mathbf{r}}{\int \epsilon^{-1}(\mathbf{r}) |D_{nk}(\mathbf{r})|^2 d\mathbf{r}} \quad (3)$$

where the integration is over a unit cell,  $D_{nk}(\mathbf{r})$  is displacement field,  $[\tilde{\epsilon}^{-1}(\mathbf{r}) - \epsilon^{-1}(\mathbf{r})]$  is nonzero, say,  $\delta$ , only at the insertion position. In our case  $\delta < 0$ , so from Eq. (3), it follows that  $\tilde{\omega}_{nk} < \omega_{nk}$ , which indicates the bands shift downwards. What is more, according to the electromagnetic variational theorem [14], the low frequency modes concentrate their energy in high  $\epsilon$  regions and the high frequency modes concentrate their energy in low  $\epsilon$  regions. The insertion of third medium ( $\epsilon > 1$ ) affects higher frequency modes more strongly, which implies that the higher frequency modes shift downwards more than the lower frequency modes.

The perturbative approach above explains a physical origin of the shift of bands in photonic crystal (PhC) slab with interlayer. However, ignoring the higher order terms, one can only obtain approximate results by Eq. (3) [13]. In this work, we use the guided-mode expansion (GME) method to calculate more accurately the electromagnetic wave propagation through the 2D dielectric lossless PPCW. GME was described in detail in a lot of papers [15, 16]. The basis of Fourier expansion, which we apply, contains 259 vectors of reciprocal lattice and 4 guided modes of the effective waveguide, which is sufficient for convergence in the calculation of photonic eigenmodes [15, 16]. So photonic eigenmodes obtained by the present approach can be considered reliable and accurate.

For simplicity, we start with the most commonly studied structure, that is W1 waveguide in an air-bridged photonic crystal slab, patterned with a triangular lattice of holes. Figure 1a shows schematic diagrams of the structure. As opposed to the general PPCW, there are additional interlayers which come from fabrication

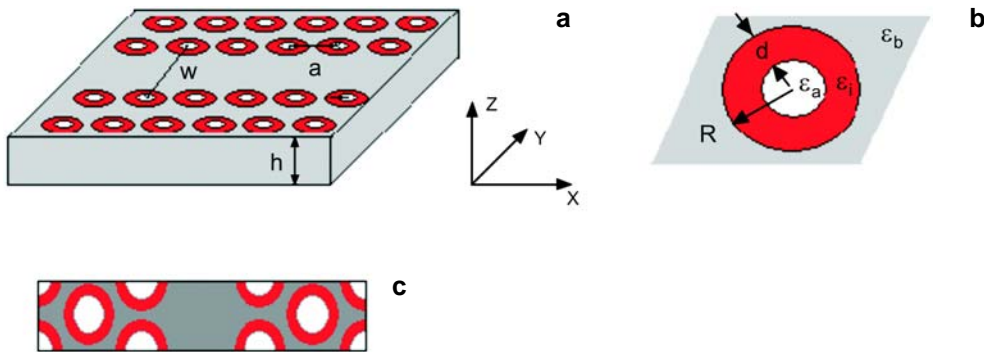


Fig. 1. Schematic picture of three-component W1 PPCW in triangular lattice of circular holes with slab thickness  $h$ , holes radius  $R$ , thickness of intermediate layer  $d$  and waveguide width ( $w = w_0 = \sqrt{3} a$ ) (a); The top view of the unit cell;  $\epsilon_a$ ,  $\epsilon_b$ ,  $\epsilon_i$  are the dielectric constant of the air holes, background and interlayer, respectively (b); The supercell for band diagram calculation using GEM method (c).

process on the inner pore's surface. One supercell with a waveguide for calculation is mapped in Fig. 1c. We define the thickness of slab to be  $h$ , the width of waveguide to be  $w$ , the thickness of interlayer to be  $d$  and denote by  $\varepsilon_b$ ,  $\varepsilon_a$  and  $\varepsilon_i$  the dielectric constant of background, air inside holes and intermediate layer, respectively. Infinite periods of the supercells are spatially repeated to form the waveguide in the  $\Gamma$ - $M$  direction. The waveguide is symmetric. Additional layer on the pore's surface is characterized by two parameters: dielectric constant  $\varepsilon_i$  and thickness  $d$ . We now restrict ourselves to the consideration of air pores  $\varepsilon_a = 1$  in the dielectric with  $\varepsilon_b = 12$ . This PPCW possesses a very large slab-mode gap for TE-like modes. The larger gap requires a larger filling factor of air holes. However, the larger filling factor of air holes will make the structure more fragile because the mechanical strength of the structure is greatly reduced. Therefore, we choose the radii of air holes to be  $0.36a$ , where  $a$  is the lattice constant. The thickness of the slab is chosen to be  $0.3a$ . The symmetry of the system is not broken by the insertion of an intermediate layer. The dielectric function of the unit crystal cell is given by [10]

$$\varepsilon(G) = \begin{cases} \frac{2\left(\frac{1}{\varepsilon_a} - \frac{1}{\varepsilon_i}\right)f_1 J_1(GR)}{GR} + \frac{2\left(\frac{1}{\varepsilon_i} - \frac{1}{\varepsilon_b}\right)f_3 J_1(G(R+d))}{G(R+d)} & G \neq 0 \\ \frac{f_1}{\varepsilon_a} + \frac{f_2}{\varepsilon_b} + \frac{f_i}{\varepsilon_i} & G = 0 \end{cases} \quad (4)$$

where  $J_1(x)$  is the Bessel function and  $f_i = \frac{2\pi}{\sqrt{3}} \frac{(R+d)^2 - R^2}{a^2}$ ,  $f_1 = \frac{2\pi}{\sqrt{3}} \frac{R^2}{a^2}$ ,  $f_2 = (1 - f_3)$ ,  $f_3 = \frac{2\pi}{\sqrt{3}} \frac{(R+d)^2}{a^2}$ .

### 3. Band diagram of guided modes

Figure 2a shows the calculated band diagram of the PPCW without interlayer for TE-like modes, the photonic mode dispersion is represented in dimensionless units  $\omega a/2\pi c$  for the frequency and  $ka/\pi$  for the wave vector. A photonic band gap (PBG) exists in the frequency range from 0.33 to 0.47 ( $\omega a/2\pi c$ ). A series of waveguide modes is formed in the PGB. The dispersion relation of the modes is understood as a mixture of two modes having different natures. One is a PBG-guided mode, which is confined by distributed Bragg reflection due to the periodic structure, and the other is an index-guided mode confined by the total internal reflection. An index-guided mode has its energy concentrated inside the defect and interacts only with the first row of holes adjacent to the defect. A gap-guided mode interacts with several rows of holes, thus it is dependent on the symmetry of the PC and its PBG. An intrinsic interaction between one gap-guided mode and one index-guided mode forms a supermode, which is

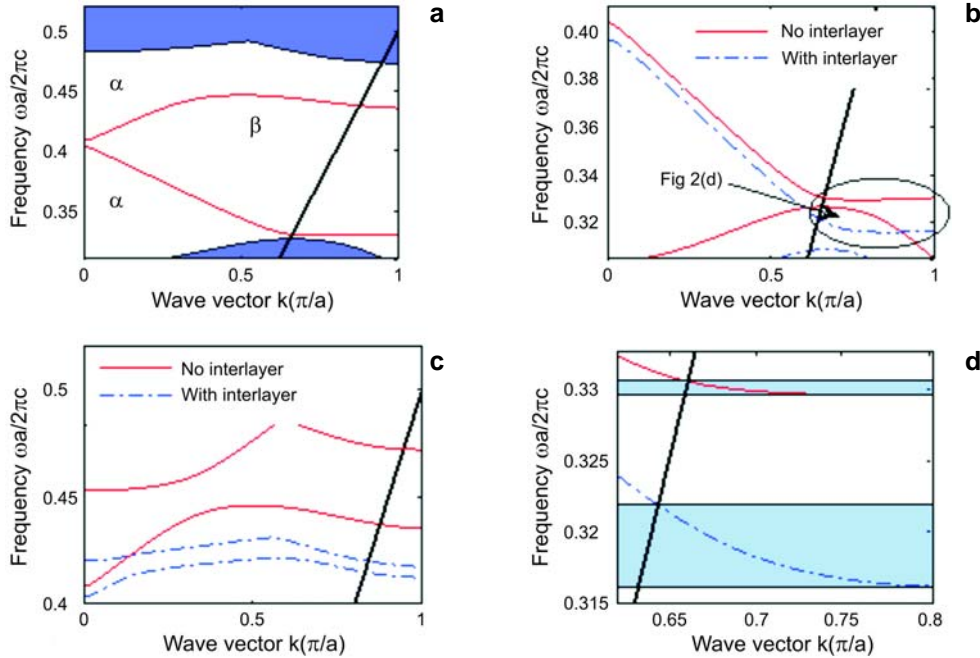


Fig. 2. Band diagram for TE-like mode of W1 air-bridge waveguide without interlayer in photonic crystal slab patterned with a triangular lattice of holes, the thick solid line is the light line of air cladding (a). Dispersion curves of the lower guided mode in PPCW with and without interlayer (b). Dispersion curves of the upper guided mode in PPCW with and without interlayer (c). The tails of the lower guided modes in part b, the frequency windows corresponding to truly guided modes are highlighted (d). The dielectric constant and thickness of interlayer are 20 and  $0.02a$ , respectively.

represented by the sum of gap-guided and index-guided mode in phase or in antiphase. In our case, four supermodes exist in the PBG region with different lateral symmetry, but only two supermodes which have even and odd symmetry with respect to reflection in the horizontal mid-plane of the channel are shown [17, 18]. We define them as the upper guided mode and the lower guided mode. The index-guided mode and gap-guided mode which interact with each other to form these two supermodes are marked as  $\alpha$  and  $\beta$ , respectively.

For the sake of clarity, the calculated band diagrams in Fig. 2 are shown only when the channel waveguide is monomode for specified parity. The thick solid line denotes the light dispersion in air cladding and every mode above this light line is leaky. When the modes cross light line of air cladding, they become true guided modes which are not theoretically subject to the intrinsic losses. What is more, as shown in Fig. 2d, the dispersion curves of the true guided modes are relatively flat, which results in a small group velocity. This small group velocity leads to a small transmission window and also means that these modes might prove to be susceptible to structural disorder, which must be present in the real samples [19]. This small group velocity can be attributed to the fact that a strong anticrossing occurs between an index-guided mode

and a gap-guided mode close to the Brillouin zone edge of W1 waveguide [1]. In the case of  $d \neq 0$  (with interlayer), due to the introduction of the extra interlayer, the guided modes shift downwards, as shown in the Figs. 1b and 1c, in which, for comparison, the corresponding bands in the case of  $d = 0$  (no interlayer) also be included. In addition, according to the electromagnetic variational theorem mentioned above, the higher the band, the greater will be its downwards shift. This is immediate obvious from comparison between two guided modes in Figs. 1b and 1c. As the guided modes shift downwards, an apparent slope in the region under the light line can be seen. The part of mode below the light line increases significantly (for example, in Fig. 2d about 5 times at  $\varepsilon_i = 20$ ). We attribute this to the fact that the introduction of the interlayer significantly shifts the anticrossing between the index-confined mode and gap-confined mode [1]. It is noticed that in a PPCW, the rearrangement of the holes in the row adjacent to the waveguide core is the usual way to achieve large transmission bandwidth for the guided modes [1, 2]. In such case, the magnification of transmission bandwidth is approximately 8 times, which is in the same order of magnification as that achieved in the structure with the interlayer discussed here (5 times). This fact demonstrates that although this additional interlayer is very thin, its effect on the PPCW is not so small as usually expected.

It is well known that the interlayer is usually very thin. According to our systematic stimulations, within a small range of interlayer thickness ( $< 0.02a$ ), the effect of interlayer depends weakly on its thickness. Therefore in this work, we only discuss structures with an interlayer thickness of  $d = 0.02a$  and with different dielectric constants.

#### 4. Group velocity and group velocity dispersion

The slow group velocity and highly dispersive nature are the most distinctive features of a linear defect waveguide. Slow light and strong dispersion will open up new possibilities for functional waveguides, so the properties such as group velocity and group velocity dispersion (GVD) of PPCW have been intensively studied since photonic crystal was found [20–22]. Group velocity of the guided modes is simply the slope of the band curve of guided modes and can be expressed as:

$$V_g = \frac{\partial \omega}{\partial k} = \frac{c}{n_g} \quad (5)$$

where  $k$  is the wave vector along the waveguide direction,  $c$  is the velocity of light in the vacuum,  $n_g$  is the group index of the dispersion material. The GVD parameter  $D$  strongly affects the propagation of optical pulse in the PPCW. Parameter  $D$  can be expressed as the second-order derivative of the dispersion relation

$$D = \frac{\partial(1/V_g)}{\partial \omega} = \frac{1}{c} \frac{\partial n_g}{\partial \omega} \quad (6)$$

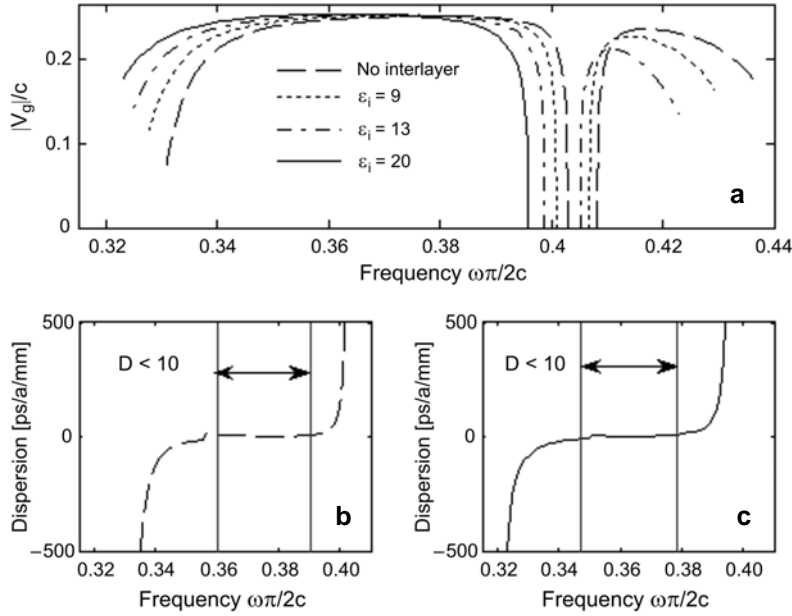


Fig. 3. Group velocity  $V_g$  in units of the speed of light in vacuum for two guided modes of PPCW with different dielectric constant of the interlayer ( $\epsilon_i = 1, 9, 13, 20$ ) (a); Group velocity dispersion parameter  $D$  of the lower guided mode of PPCW without interlayer (b); Group velocity dispersion parameter  $D$  of the lower guided mode of PPCW with interlayer ( $\epsilon_i < 20$ ) (c). In parts b and c two vertical lines represent the boundaries of frequency range corresponding to  $D < 10$ .

Figure 3 shows the group velocities and the GVD of the waveguide modes with respect to the normalized frequency. In the central region, the linear defect waveguide exhibits relatively high group velocity, and the dispersion value  $D$  changes almost linearly. Around the band edges the group velocity is very low and as a result the GVD changes sharply there, toward positive values at one edge and negative values at the other.

Generally speaking, the origin of low group velocity in PPCW is related to three different physical effects [23]:

- The conventional distributed feedback (DFB) effect, which is a coupling between a forward and a backward mode with the same lateral field distribution.
- The DFB effect between a PBG-guided mode and an index-guided mode, which occurs at the anticrossing point.
- Omnidirectional reflection which is a unique feature offered by the photonic crystal environment.

In PPCW, a photonic band gap is presented, light propagating at any angle is reflected in the lateral direction to the waveguide and thus has large lateral wave vector components along the direction perpendicular to the waveguide and in the plane of the slab. Therefore, wave vector components parallel to the waveguides are

negligible near  $k \approx 0 \times 2\pi/a$ . This indicates that the two supermodes in Fig. 3a have low group velocity near  $k \approx 0 \times 2\pi/a$  [23].

In the W1 waveguide, an anti-crossing between a PBG-guided mode and an index-guided mode occurs close to the Brillouin zone edge ( $k \approx 0.5 \times 2\pi/a$ ) [24], which results in slow light near the point. The introduction of the interlayer increases the effective dielectric constants in the core part of PPCW locally, the index-guided and gap-guided modes move downwards but the gap-guided mode moves faster and thus, anticrossing near the Brillouin zone edge is canceled. Only DFB plays a major role in slowing light, the group velocity becomes higher. This is confirmed by what happens in lower frequency region of the lower guided mode in Fig. 3a. However, near the point  $k \approx 0 \times 2\pi/a$ , a photonic-band-guided mode, which forms the left part of the upper edge of PBG [17], comes closer to the upper guided mode (an index-guided mode), and the coupling between them becomes stronger, which results in lower group velocity in the higher frequency region of the upper guided mode in Fig. 3a.

The introduction of interlayer changes the dielectric constant of PPCW, the eigenfrequency shifts to lower frequency, the change in the eigenfrequency causes a shift of both the group velocity curve and the dispersion curve to lower frequency region. The central gentle inclination region is suitable for device application due to quasi-linear dispersion. In the PPCW without interlayer, the range of bandwidth within which the dispersion is below 1 (ps/a/mm) is  $0.0038(\omega a/2\pi c)$  (from 0.3778 to 0.3816  $\omega a/2\pi c$ ) and increases to 0.03 ( $\omega a/2\pi c$ ) (from 0.3604 to 0.3903  $\omega a/2\pi c$ ) for less strict constraint of the dispersion 10 (ps/a/mm). While in the corresponding PPCW with interlayer ( $\varepsilon_i = 20$ ) they are 0.005  $\omega a/2\pi c$  (from 0.3686 to 0.3737  $\omega a/2\pi c$ ) and 0.0314 ( $\omega a/2\pi c$ ) (from 0.3536 to 0.3849  $\omega a/2\pi c$ ), respectively. It is clear that the introduction of an interlayer results in a broadening of the bandwidth corresponding to certain dispersion region and a downward shift of its frequency region. The rate of frequency shift to bandwidth for  $D < 1$  and  $D < 10$  is 1.3421 and 0.2267, respectively. In a high-bit-rate WDM optical communication system, signal pulses, after having been de-multiplexed, are individually reshaped in each channel where a tunable dispersion compensator is required precisely to compensate for dispersion. The group velocity dispersion performances of a PPCW strongly depends upon precise wavelength matching. The introduction of an interlayer causes a downward shift of dispersion curve to lower frequencies, thus lowering operation frequency's dispersion value from its original position factored into the device's design [20]. This results in a mismatch between the manufacturer's compensation value and device's actual dispersion wave frequency, owing to excessive or insufficient compensation. Naturally, the consequences of this mismatch would be more pronounced at frequencies along the band edges where as our results show, dispersion values increase or decrease exponentially (see Figs. 3b and 3c). Clearly, then, the influence of added interlayer on the dispersive nature of a given PPCW must be carefully taken into consideration.



## 5. Intrinsic loss of guided modes

The introduction of an interlayer results in the decrease in the hole radius, so the part of electric field scattering out into air decreases and the intrinsic losses decrease [25, 26]. In order to see clearly the influence of interlayer on the intrinsic losses, for different dielectric constants of the interlayer, the intrinsic losses are computed and plotted in Fig. 4. From Fig. 4, it can be observed that as dielectric constant of the interlayer increases, the intrinsic loss of the guided modes reduces in the frequency region of

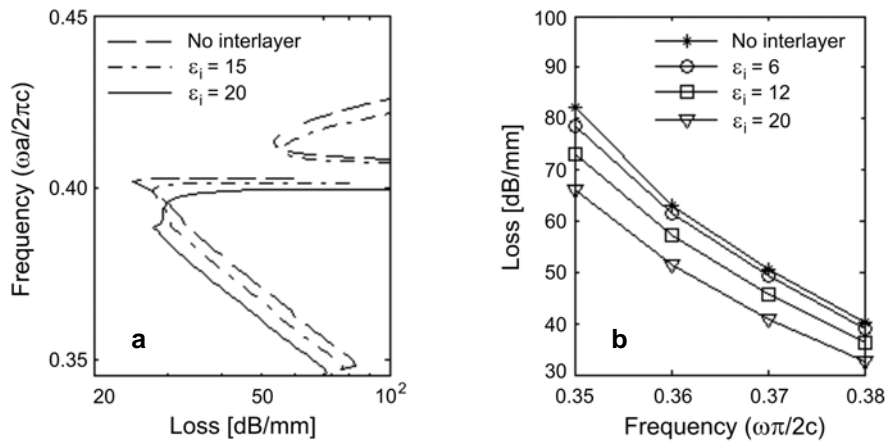


Fig. 4. Propagation losses of both guided modes of PPCW with different dielectric constants of the interlayer (a). In frequency region of higher group velocity, propagation losses of lower guided mode of PPCW with different dielectric constants of the interlayer (b).

high group velocity of the guided mode. For example, at  $\omega = 0.36$ , the introduction of the interlayer with  $\epsilon_i$  (equal to 6, 12, 20) reduces the intrinsic loss by 3.65, 9.15, 16 dB/mm. Compared to the propagation loss (usually  $< 10$  dB/mm) in many kinds of PPCW which have been optimized by various methods [27, 28] the change in loss which comes from the introduction of an interlayer is not insignificant. In some real PPCWs (which have been optimized to some extent), in order to accurately evaluate the impact of optimized methods on propagation losses, the positive impact on losses which the addition of an interlayer brings about has to be taken into account [27, 28].

## 6. Sensitivity of the effect of an intermediate layer to waveguide width and slab thickness

From the discussion above, one can see that the introduction of an interlayer definitely influences the properties of PPCW. However, for prospective application,

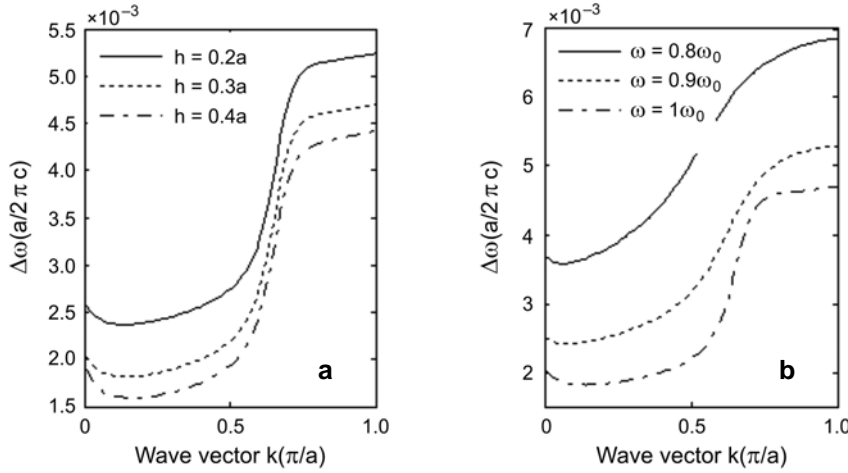


Fig. 5. The amount of frequency shift for lower guided mode in PPCW with different slab thickness (a). The amount of frequency shift for lower guided mode in PPCW with different waveguide width (b).

it is necessary to analyze the sensitivity of properties of PPCW to interlayer to obtain a more fabrication tolerant PPCW. Figure 5 shows the amount frequency shift for the lower guided mode  $\Delta\omega = \omega - \omega_0$  ( $\omega$  is the eigenfrequency of the lower guided mode in PPCW with interlayer,  $\omega_0$  is the corresponding eigenfrequency of the lower guided mode in PPCW without interlayer), which is brought about by the introduction of the interlayer with different dielectric constants. For simplicity of analysis, we choose right parameters which ensure the two guided modes being in the PBG entirely, we find that the narrower is a waveguide in a thinner slab, the greater is the impact. So, PPCW with wider waveguide width and thicker slab thickness is more tolerant to interlayer. It is noticed that for different frequency range of guided mode, the amount of frequency shift is different. The lower is the frequency, the higher is the shift. This is because in the lower frequency region, the guided modes have a lower group velocity, and a slow mode experiences a larger change in the effective index than a fast mode, despite the fact that the change in the material index  $\Delta n$  is the same [23].

## 7. Conclusions

We present a comprehensive study about the role of interlayer in the three-component PPCW. We first calculate the band diagram, intrinsic loss, group velocity and group velocity dispersion of PPCW with and without interlayer using GME method. Due to the introduction of the interlayer, the single-mode transmission window of the lower guided mode is substantially widened. The intrinsic losses of guided modes decrease in frequency region of higher group velocity. The group velocity and the group velocity dispersion curve definitely shift to lower frequencies. In prospective application of

PPWCs, the performances of which strongly depend upon precise wavelength matching, the effect of the interlayer has to be taken into consideration.

*Acknowledgements* – This research was supported by the NSFC (No. 60707001, No. 60711140087), National 973 Program (No. 2007CB310705), National 863 Program (No. 2007AA01Z247), NCET (07-0110), PCSIRT (No. IRT0609), ISTCP (No. 2006DFA11040), 111 Project (No. B07005) P.R. China.

## References

- [1] YAMADA K., MORITA H., SHINYA A., NOTOMI M., *Improved line defect structures for photonic crystal waveguides with high group velocity*, Optics Communications **198**(4–6), 2001, pp. 395–402.
- [2] SHINYA A., NOTOMI M., KURAMOCHI E., *Single-mode transmission in commensurate width-varied line-defect SOI photonic crystal waveguides*, Proceedings of SPIE **5000**, 2003, pp. 125–135.
- [3] NOTOMI M., YAMADA K., SHINYA A., TAKAHASHI J., TAKAHASHI C., YOKOHAMA I., *Extremely large group-velocity dispersion of line-defect waveguides in photonic crystal slabs*, Physical Review Letters **87**(25), 2001, p. 253902.
- [4] HUGHES S., RAMUNNO L., YOUNG J.F., SIPE J.E., *Extrinsic optical scattering loss in photonic crystal waveguides: role of fabrication disorder and photon group velocity*, Physical Review Letters **94**(3), 2005, p. 033903.
- [5] CHUTINAN A., NODA S., *Waveguides and waveguide bends in two-dimensional photonic crystal slabs*, Physical Review B: Condensed Matter **62**(7), 2000, pp. 4488–4492.
- [6] TANAKA Y., ASANO T., AKAHANE Y., SONG B.S., NODA S., *Theoretical investigation of a two-dimensional photonic crystal slab with truncated cone air holes*, Applied Physics Letters **82**(11), 2003, pp. 1661–1663.
- [7] GERACE D., ANDREANI L.C., *Disorder-induced losses in photonic crystal waveguides with line defects*, Optics Letters **29**(16), 2004, pp. 1897–1899.
- [8] GERACE D., ANDREANI L.C., *Low-loss guided modes in photonic crystal waveguides*, Optics Express **13**(13), 2005, pp. 4939–4951.
- [9] JOHNSON S.G., POVINELLI M.L., SOLJACIC M., KARALIS A., JACOBS S., JOANNOPOULOS J.D., *Roughness losses and volume-current methods in photonic-crystal waveguides*, Applied Physics B: Lasers and Optics **81**(2–3), 2005, pp. 283–293.
- [10] GLUSHKO A., KARACHEVTSEVA L., *PBG properties of three-component 2D photonic crystals*, Photonics and Nanostructures: Fundamentals and Applications **4**(3), 2006, pp. 141–145.
- [11] TRIFONOV T., MARSAL L.F., RODRIGUEZ A., PALLARES J., ALCUBILLA R., *Analysis of photonic band gaps in two-dimensional photonic crystals with rods covered by a thin interfacial layer*, Physical Review B: Condensed Matter **70**(19), 2004, p. 195108.
- [12] THITSA M., SONG Y., ALBIN S., *Effect of oxidation, etching, and thin-film deposition on silicon photonic crystals*, Journal of the Electrochemical Society **155**(6), 2008, pp. H351–H356.
- [13] ZHANG X., ZHANG Z., LI L., JIN C., ZHANG D., MAN B., CHENG B., *Enlarging a photonic band gap by using insertion*, Physical Review B: Condensed Matter **61**(3), 2000, pp. 1892–1897.
- [14] JOANNOPOULOS J.D., MEADE R.D., WINN J.N., *Photonic Crystals: Molding the Flow of Light*, Princeton, Princeton University Press, NJ, 1995.
- [15] ANDREANI L.C., AGIO M., *Photonic bands and gap maps in a photonic crystal slab*, IEEE Journal of Quantum Electronics **38**(7), 2002, pp. 891–898.
- [16] ANDREANI L.C., GERACE D., *Photonic-crystal slabs with a triangular lattice of triangular holes investigated using a guided-mode expansion method*, Physical Review B: Condensed Matter and Materials Physics **73**(23), 2006, pp. 235114/1–16.

- [17] ANDREANI L.C., AGIO M., *Intrinsic diffraction losses in photonic crystal waveguides with line defects*, Applied Physics Letters **82**(13), 2003, pp. 2011–2013.
- [18] LETARTRE X., SEASSAL C., GRILLET C., ROJO-ROMEO P., VIKTOROVITCH P., LE VASSOR D'YERVILLE M., CASSAGNE D., JOUANIN C., *Group velocity and propagation losses measurement in a single-line photonic-crystal waveguide on InP membranes*, Applied Physics Letters **79**(15), 2001, pp. 2312–2314.
- [19] NOTOMI M., SHINYA A., YAMADA K., TAKAHASHI J.-I., TAKAHASHI C., YOKOHAMA I., *Structural tuning of guiding modes of line-defect waveguides of silicon-on-insulator photonic crystal slabs*, IEEE Journal of Quantum Electronics **38**(7), 2002, pp. 736–742.
- [20] HOSOMI K., KATSUYAMA T., *A dispersion compensator using coupled defects in a photonic crystal*, IEEE Journal of Quantum Electronics **38**(7), 2002, pp. 825–829.
- [21] SAYNATJOKI A., MULOT M., AHOPELTO J., LIPSANEN H., *Dispersion engineering of photonic crystal waveguides with ring-shaped holes*, Optics Express **15**(13), 2007, pp. 8323–8328.
- [22] PETROV A.YU., EICH M., *Zero dispersion at small group velocities in photonic crystal waveguides*, Applied Physics Letters **85**(21), 2004, pp. 4866–4868.
- [23] KRAUSS T.F., *Slow light in photonic crystal waveguides*, Journal of Physics D: Applied Physics **40**(9), 2007, pp. 2666–2670.
- [24] PETROV A.YU., EICH M., *Dispersion compensation with photonic crystal line defect waveguides*, IEEE Journal on Selected Areas in Communications **23**(7), 2005, pp. 1396–1401.
- [25] KAFESAKI M., SOUKOULIS C.M., AGIO M., *Losses and transmission in two-dimensional slab photonic crystals*, Journal of Applied Physics **96**(8), 2004, pp. 4033–4038.
- [26] BENISTY H., LABILLOY D., WEISBUCH C., SMITH C.J.M., KRAUSS T.F., CASSAGNE D., BERAUD A., JOUANIN C., *Radiation losses of waveguide-based two-dimensional photonic crystals: Positive role of the substrate*, Applied Physics Letters **76**(5), 2000, pp. 532–534.
- [27] O'FAOLAIN L., YUAN X., MCINTYRE D., THOMS S., CHONG H., DE LA RUE R.M., KRAUSS T.F., *Low-loss propagation in photonic crystal waveguides*, Electronics Letters **42**(25), 2006, pp. 1454–1455.
- [28] TANAKA Y., SUGIMOTO Y., IKEDA N., NAKAMURA H., ASAKAWA K., INOUE K., JOHNSON S.G., *Group velocity dependence of propagation losses in single-line-defect photonic crystal waveguides on GaAs membranes*, Electronics Letters **40**(3), 2004, pp. 174–176.

*Received August 4, 2008  
in revised form October 28, 2008*